Annual and seasonal precipitation trends and their attributions in the Qinling Mountains, a climate transitional zone of China

Meng, Q. and Bai, H. and Sarukkalige, R. and Fu, G. and Jia, W. and Zhang, C.

Abstract

Trends of annual and seasonal precipitation and their linkage with large-scale climate indices were investigated in this study with the Innovative Trend Analysis (ITA) methods for the Qingling Mountains (QMs), using 32 meteorological stations' monthly observed precipitation from 1959 to 2016. The results indicated that a declining trend of annual precipitation was found in the QMs. Seasonally, a decreasing trend was also found during spring and autumn, while an increasing trend was observed in summer and winter. Spring and autumn precipitation were the contributors to the decline of annual precipitation. More important, both low values and high values indicated a reduction trend, which would have essential impacts on ecology and people's life in the QMs. The results of wavelet coherence showed that annual precipitation had strong linkages with EASMI, SOI, SASMI, SCSMI and SWACI, and had an insignificant relationship with NAO and WASMI. Seasonally, EASMI had negative effects on each season. Spring and autumn precipitation was more sensitive to SOI than SWACI, while SASMI had a strong positive relationship with winter precipitation and SCSMI was more negatively related to autumn and winter precipitation.

Key words: precipitation; climate change; ITA; trend analysis; Qinling Mountains

1 Introduction

Precipitation is one of the basic meteorological factors and one of the primary components of hydrological cycles. Precipitation significantly influences not only on water resources utilization and flood warning, but to human health (Yang et al. 2016). Meanwhile, global warming is an indisputable fact (Mohan et al. 2018). Global annual precipitation has increased from 1951 to 2010, and unlike temperature, it has existed spatial inconsistency globally (IPCC, 2014). Especially in China where the land area is vast and the terrain is rugged. A numerous number of studies suggested that annual precipitation has increased in southeast China (Li et al. 2016; Wu et al. 2016), while decreased in southwest China (Cheng et al. 2019; Yu et al. 2018). Peculiarly, annual precipitation in northwest China displays both an increasing trend and a decreasing trend in some investigations (Han et al. 2016; Hao et al. 2017; Wang et al. 2019; Li et al. 2016; Fu et al. 2004). Furthermore, a preponderance of studies suggested that climate change is more rapid in the mountainous regions (Li et al. 2012; Li et al. 2013; Li et al. 2011). QMs is located in Shaanxi province in northwest China. As a transitional zone of China, this area is vulnerable to climate change, and floods are one of the major natural hazards in this area. The flood in 2002, for example, resulted in more than 400 death and significant economical loss in the southern slope of the QMs (Li 2003). Studying the precipitation in the mountainous area could further understand the global warming and hydrological cycle regionally which is more useful for identifying climate change adaption options, particularly in water resources management.

The aforementioned investigations of precipitation trends were all tested by different classical trend methods. However, these methods could not detect the low, medium and high values of one geographical variable. Therefore, a new trend method named Innovative trend analysis (ITA) proposed by Şen (2012) to explore different values of one time series (Dabanlı et al. 2016). Variation of seasonal precipitation has to be vital on vegetation and crop growth. Qin et al. (2017) found that the temperature in spring and summer is the dominant factor for the radial growth of trees, and excessive precipitation in winter would slow down tissue growth. Proud and Rasmussen (2011) found that plant growth may be stunted if it encounters a drought during the onset of growth. The precipitation is closely influenced by climate anomalies which provide a macro climate background.

Therefore, in order to study the trend of annual and seasonal precipitation and its attributions under the impacts of climate change in the QMs, this study applied the ITA method to detect the trend of precipitation and its hidden values, and chose 15 large - scale climate anomalies indices aiming to analyze the connection with precipitation in the QMs. This study will provide recommendations and guidelines to enhance the scientific basis for forecasting of precipitation, prevention and mitigation of flood in the future.

2 Data and Method

2.1 Study area

Qinling Mountains (32° 54′ - 34° 35′ N， 105° 30′ - 111° 3′ E) is located in Shaanxi Province in central China. QMs carries a total area of 61,900 km^2

(Fig. 1). QMs is a typical climate transitional zone in China – the dividing line of South and North China, the 0 °C isotherm in January and the 800mm annual precipitation isohyet, the watershed of the Yellow and Yangtze River (Deng et al. 2019), the boundary between northern wheat and southern rice, the border of rivers to ice period, the boundary between Loess Plateau and Sichuan Basin. The peak of QMs is Mount Taibai, with an elevation of 3771.2m, which could block the cold current from North, the land of abundance in Sichuan was created. Specially, since it is also the climate transition belt in China where the typical subtropical zone changes gradually toward the warm temperate zone from south to north and the humid zone fluctuates continuously toward the semi-humid zone from east to west (Deng et al. 2019). The average annual precipitation is approximately 825mm, and over 70% of precipitation occurs during the monsoon period from May to September (Guo et al. 2018). The south region receives the highest annual precipitation of 1156mm, while the northern region receives 545mm average precipitation annually (Meng et al. 2019). The annual precipitation decreases from southern part to northern part of the QMs.

2.2 Data sources

Monthly precipitation records covered from 1959 to 2016 from 32 rain gauge stations collected from the Shaanxi Meteorological Bureau. Then, March to May represented as spring, June to August summer, September to November autumn and December to February winter.

The large-scale climate indices: Atlantic Oscillation (AO) is obtained from the NOAA National Climatic Data Center (http://www.ncdc.noaa.gov/teleconnections/ao.php), and Pacific Decadal Oscillation (PDO) index from the National Climate Center of China (NCC) (http://cmdp.ncc-cma.net/cn), East Asian Summer Monsoon Index (EASMI), Southern Oscillation Index (SOI), South Asian Summer Monsoon Index (SASMI), South China Sea Summer Monsoon Index (SCSMI), North Atlantic Oscillation (NAO), Atlantic Multi-decadal Oscillation (AMO), North American Summer Monsoon Index (NASMI), Pacific North American Pattern (PNA), Australian Summer Monsoon Index (AUSMI), Monsoon like Southwest Australian Circulation Index (SWACI), South American Summer Monsoon Index (SHAMI), West African Summer Monsoon Index (WASMI) and South Atlantic Ocean Dipole Index (SAODI) (http://ljp.lasg.ac.cn/dct/page/.) were used to represent large-scale climate anomalies. They are all used to study the relationship between atmospheric circulations and precipitation.

2.3 Methodology

2.3.1 Innovative Trend Analysis (ITA)

Innovative Trend Analysis (ITA) was proposed by Sen (2012) firstly, which could be used for trend analysis in the hydrometeorology time series, such as: temperature (Mohorji and Sen 2017), precipitation (Öztopal and Sen 2017) and pan evaporation (Kisi 2015). In the innovative trend analysis, the given time series is divided into two equal parts and then each part is ordered ascendingly. Plot the two parts in a scatter plot, and then plot the 1:1 line, and finally, divide the X axis into three parts ("Low" < 10th percentile, "Medium" = 10th – 90th percentile and "High" > 90th percentile). Fig. 2 clearly shows the ITA. There is no trend if the precipitation time series fall exactly or approximately around the vicinity of 1:1 straight line. It means an increasing trend in the case that scatter points fall over the 1:1 line. Otherwise, it is a decreasing trend if the scatter points accumulated below the 1:1 line,. The slope of ITA can be expressed as below (Sen 2017).

$$s = \frac{2(\bar{y}_2 - \bar{y}_1)}{n} \quad (1)$$

Where $\bar{y}_1$ represents the precipitation series from 1959 to1987, and $\bar{y}_2$ represents the precipitation series from 1988 to 2016, and n is 58 in this paper.

2.3.2 Wavelet analysis

Wavelet coherence (WTC) was applied to study the relationship between precipitation and large climate anomalies in many literatures (Xuhu Wang et al. 2019; Grinsted et al. 2004). The wavelet coherence could be expressed as follows (Torrence and Webster, 1999):

$$R_n^2(s) = \frac{\left|S\left(s^{-1}W_n^{XY}(s)\right)\right|^2}{S\left(s^{-1}\left|W_n^X(s)\right|^2\right) \times S\left(s^{-1}\left|W_n^Y(s)\right|^2\right)} \quad (2)$$

Where two time series X and Y with transform W_n^X and W_n^Y, S is a smoothing operator, could be expressed as below:

$$S(W) = S_{scale}\left(S_{time}\left(W_n(s)\right)\right), \quad (3)$$

The WTC uses Monte Carlo methods with red noise to determine the 5% statistical significance level of the coherence (Jevrejeva et al., 2003).

3 Results

3.1 Trend analysis of precipitation in the QMs

3.1.1 Annual trend of precipitation

The ITA method is applied to analyze the annual precipitation from 1959 to 2016. The result of the trend in annual precipitation tested by the ITA method indicated that majority of the stations showed a slightly declining trend (Fig. 3). Specifically, 30 out of 32 stations revealed a decreasing trend, while like Lueyang station in Fig. 3, Shangnan station also showed an insignificant increasing trend. Fig 3 shows only three stations as representative results (Lueyang, Changan and Huashan station), where the other stations which have the same trend at the same time without other characteristics like Changan station. Huashan, as the station with highest elevation (2065m), had the biggest decline trend slope of -5.1mm/year. The relationship between the ground elevation and slope of the trend demonstrates that trend slope has an insignificant relationship with the elevation except for Huashan station (Fig.4). Additionally, 30 out of 32 stations of the high value (90^{th} percentile as in the Fig. 2) showed a declining trend, which implied less probability of floods in the near future. This finding was consistent with the trend tested by the M-K method of annual precipitation in the Yellow River in the northwest China which most of the stations showed a decreasing trend, while few stations indicated an increasing trend (Liu et al. 2008; Xu et al. 2007).

3.1.2 Seasonal trend of precipitation

Trend in seasonal precipitation assessed by the ITA method indicated that an obvious seasonal trend (Fig. 5-8.). 30 out of 32 the stations exhibited an insignificant decreasing trend except for two stations: Huayin and Chenggu which showed an upturn trend in spring (Fig. 5). As the highest station, Huashan has the biggest decreasing slope of -1.83mm/year. The other stations with the same trend as Changan station are not presented in this figure to save the space. The trend in summer was complicated as shown in Fig. 6. 11 stations similar with Xunyang station showed a dwindling trend and other 21 stations similar to Changan station exhibited an increasing trend, and Shangnan station had the biggest increasing trend slope of 1.95mm/year. (Other stations were not shown in the figure). Autumn precipitation was dominated by negative trend except for Chenggu and Lueyang stations which showed a positive trend (Fig. 7). Ziyang station had the biggest decreasing trend slope of -3.2mm/year. The other stations show negative trend similar to the trend as Huashan station, hence only Huashan station was presented in Fig. 7. As shown in Fig.8, it showed an insignificant increment trend for most of the stations in winter except Xunyang, Zhashui (not shown in Fig. 8) and Ziyang (not shown in Fig. 8) stations which showed a declining trend, and Lueyang station had the biggest increasing trend slope of 0.94mm/year. The other stations followed the same trend as Shangnan station.

Further analysis declared that the reason for decreasing annual precipitation is dominated by decreasing spring and autumn precipitation. Importantly, most of the low precipitation values (10^{th} percentile as in the Fig. 2), especially in spring showed a decreasing trend which had a trend of the drier condition and inverse influences on crops and vegetation growth. Most of the high precipitation values (90^{th} percentile as in the Fig. 2) in summer indicated a decreasing trend which has advantage of floods control, especially in the flood-prone area at the southern slope of the QMs. This finding is the same with Zhang's results tested by M-K method which implies a risk of droughts can be expected in spring and autumn, and precipitation increased in winter and summer in the Yellow River basin in the northwest China (Zhang et al. 2014).

3.2 Influence of Climate Index on Precipitation

3.2.1 Climate Index on annual precipitation

The correlation analysis between annual precipitation of the 32 stations and climate indices was shown in Fig. 9. This result indicates that the impact of climate indices on annual precipitation was different in different places. It can be found that SOI, SAODI and SWACI had a strong positive relationship with annual average precipitation among all the stations. Conversely, EASMI, SCSMI and SASMI had a negative relationship with annual average precipitation. In addition, the positive relationship was stronger than the negative relationship.

QMs locates in the monsoon area of China, are vulnerable to climate circulation indices from all over the world. The wavelet coherence showed that there was a correlation between precipitation and climate indices (Fig. 10). In addition Fig.10 (a) shows that similar to SOI and SWACI, PNA, AO, SAODI and SHAMI had a significant positive correlation with annual average precipitation. These six indices all had an impact on annual precipitation during the 1980s - 1990s with different scales. Additionally, SOI and SWACI had a more coherent relationship with annual precipitation. Conversely, SCSMI had a significant negative correlation in 1978 - 1994 and 1998 - 2006, respectively (Fig. 10b).

There was a significant positive and negative correlation of SASMI, NASMI and AUSMI, and these three indices all had the impact during the 1990s - 2000s. Unlike the other two indices, SASMI (Fig. 10c) had the strongest correlation with the scale of 2 -

4 years and 2 - 8 years in 1966 - 1971 and 1977 - 2006, respectively.

Furthermore, it can be seen that a significant positive correlation of AMO during 1978 - 1987 and a significant lagged correlation during 2000 - 2003 (Fig. 10d). EASMI had a significant negative influence on precipitation on the scale of 1 - 3 years and 4 - 8 years in 1998 - 2002 and 1982 - 2008, and a significant lagged influence on the scale of 2 - 3 years during 1979 - 1981 (Fig. 10e). PDO had little coherence with annual precipitation (Fig. 10f). Lastly, it can also be observed that like NAO, WASMI had an insignificant impact on annual average precipitation (Fig. 10g). Other research indicated that El Nino and La Nina also could affect the climate in the Yellow River basin, even in east China (Fu et al. 2007; Wang et al. 2000).

3.2.2 Climate Index on seasonal precipitation

Annual precipitation had strong linkages with EASMI, SOI, SASMI, SCSMI and SWACI based on the significant area from Fig. 10. Therefore, the effect of five climate indices on seasonal precipitation was shown in Fig. 11. It showed that EASMI had the most significant negative and lagged relationship in summer from 1980 to 2008, and had a negative relationship in spring in the 1980s. A significant positive relationship was found in winter in the 1990s. Furthermore, the plot also indicated that the linkage between EASMI and autumn precipitation was inconsistent.

Fig. 11b and 11e indicated that SOI and SWACI had a more significant connection with spring and autumn precipitation, and SWACI and SOI with summer and winter precipitation showed small areas of significant coherence. There was a significant negative and positive cycles from 1990 to 2000 in spring of SOI, and had a positive cycle in the 1988s and 2000s in autumn. There was a lagged relationship with spring precipitation from 1968 to 1990 and ahead of SWACI in the 1990s. SWACI had a positive relationship with precipitation in the 1990s in autumn. Also it demonstrated that SOI was stronger than SWACI (Fig. 11b and Fig. 11e).

SASMI had a strong positive relationship with winter precipitation in the 1980s in Fig. 11c. Fig. 11d revealed that SCSMI had more coherence with autumn and winter precipitation. There was a lagged relationship between SCSMI and winter precipitation from 1972 to 1992, and a positive relationship from 1975 to 2000. From 1982 to 1990, SCSMI was negatively related to autumn precipitation (Fig.11e).

4 Discussion

The annual precipitation trend tested by ITA in this study has the same result as a linear regression method drawn by Bai et al. (2019) in the QMs. Some findings suggested a general decreasing trend was found in Shaanxi province in northwest China (Han et al. 2016; Hao et al. 2017; Wang et al. 2019), while others (Li et al. 2016) agreed that an increasing trend was found in northwest China. As there is not a clear boundary of northwest China, it would be an increasing trend of annual precipitation when excluded the QMs. Annual precipitation indicated a decreasing trend including the QMs. This clearly illustrates the importance of the Qinling Mountains in determining the trend of annual precipitation in the area.

In this study, the investigation suggested that annual and seasonal precipitation influenced by climate anomalies in the QMs. EASMI as the most significantly influenced factors, it has had an impact on many places in China, such as Loess plateau (Wang X et al. 2019) and northwest China (Li B et al. 2016). SOI as the second factor which has influenced the precipitation in the QMs. SOI is the index of ENSO event, the same with El Nino and La Nina, they have some impacts on precipitation in some regions in China. Meanwhile, this conclusion is consistent with many studies (Li B et al. 2016; Fu et al. 2007), indicating that EASMI and SOI as the most influencing factors, should be taken into account when forecasting the precipitation in this area. Many investigations have also agreed that PDO has a varying degree impact on precipitation in different regions in China (Xiao et al. 2015; Zhang et al. 2017; Yang et al. 2017; Fu et al. 2009), but in this study, wavelet coherence result showed that PDO had little coherence with annual precipitation. A possible reason could be the complicated mechanism between PDO and East Asian winter monsoons. Apart from large atmospheric circulation anomalies, temperature, topography and human activities all might be the factors attributes to the variation of precipitation in this area. It should study the relationship between these factors and precipitation, and to be taken into account when forecasting the future precipitation in the QMs.

The advantage of ITA is that the high values (90^{th} percentile) could be easily observed, which is helpful to spot the trends in extreme values (Dabanlı et al., 2016; Şen, 2017). In this way, Ministry of agriculture and Disaster bureau could identify trends for different precipitation categories by ITA (Wang et al., 2020). Mostly all the low values (10^{th} percentile), especially in spring showed a declining trend, which had an inverse influence on crop and vegetation growth. If this trend continues in the future, the shortage of water resources would be aggravated and resulted in a serious reduction in agricultural output.

The primary problem in this study is the limited number of hydrological observation stations in the QMs mountainous area and of its complex topography. As for the influencing factors of this area, it is hard to analyze all the human and natural factors to the precipitation in the QMs. Further studies should focus on these aspects aiming to gain more accurate trends and attribution analysis.

5 Conclusion

The trend of annual and seasonal precipitation in the Qinling Mountains (QMs) was investigated, using 32 meteorological stations' monthly observed precipitation from 1959 to 2016. And the effect of climate index on annual and seasonal precipitation was evaluated, using ITA trend method and wavelet coherence. The conclusions were made as follows.

Annual precipitation showed a decreasing trend at most of the stations in the QMs from 1959 to 2016. Seasonally, a decreasing trend was also found during spring and autumn, while an increasing trend was observed in summer and winter. Additionally, the larger part of the low and high values, showed a decreasing trend which is a vital warning to the environment, ecosystem and agriculture. Thus, much more attention should be paid in this area.

EASMI, SOI, SASMI, SCSMI and SWACI are the most influencing factors that have an impact on annual and seasonal precipitation, while NAO and WASMI had an insignificant relationship with precipitation in the QMs. This should be taken into account when forecasting the precipitation in the future in this area.

References

Bai, H.Y., Liu, K., Wang, J., Li, S.H., 2019. Response and Adaptation of Vegetation in Qinling Mountains under Climate Change. Science Press. Beijing 58-61. (in Chinese)

Cheng, Q., Gao, L., Zuo, X., & Zhong, F., 2019. Statistical analyses of spatial and temporal variabilities in total, daytime, and nighttime precipitation indices and of extreme dry/wet association with large-scale circulations of Southwest China, 1961–2016. Atmos Res. 219, 166-182.

Dabanlı, İ., Şen, Z., Yeleğen, M.O., Şişman, E., Selek, B., Güçlü, Y., 2016. Trend assessment by the innovative-Şen method. Water Resour Manag 30 (14), 1–11.

Deng, C., Bai, H., Ma, X., Zhao, T., Gao, S., & Huang, X., 2019. Spatiotemporal differences in the climatic growing season in the Qinling Mountains of China under the influence of global warming from 1964 to 2015. Theor Appl Climatol. 138(3-4): 1899-1911.

Fu, G., Chen, S., Liu, C., & Shepard, D., 2004. Hydro-climatic trends of the Yellow River basin for the last 50 years. Climatic Change. 65(1-2), 149-178.

Fu, G., Charles, S.P., Viney, N.R., Chen, S., & Wu, J. Q., 2007. Impacts of climate variability on stream‐flow in the Yellow River. Hydrol Process. 21(25), 3431-

3439.

Fu, G., Charles, S.P., Yu, J., & Liu, C., 2009. Decadal climatic variability, trends, and future scenarios for the North China Plain. J Climate. 22(8), 2111-2123.

Grinsted, A., Moore, J.C., Jevrejeva, S., 2004. Application of the cross wavelet transform and wavelet coherence to geophysical time series. Nonlin Process Geophys 11 (5/6), 561–566.

Guo, S.H., Bai, H.Y., Meng, Q., 2018. Landscape pattern change and its response to human disturbance in Qinling region from 1980 to 2015. J. Appl Ecol. 29, 4080–4088. (in Chinese)

Han, X., Xue, H., Zhao, C., Lu, D., 2016. The roles of convective and stratiform precipitation in the observed precipitation trends in Northwest China during 1961–2000. Atmos Res. 169, 139–146.

IPCC, 2014: Climate Change 2014: Synthesis Report. Contribution of Working Groups I, II and III to the Fifth Assessment Report of the Intergovernmental Panel on Climate Change [Core Writing Team, R.K. Pachauri and L.A. Meyer (eds.)]. IPCC, Geneva, Switzerland, 151 pp.

Jevrejeva, S., Moore, J.C., Grinsted, A., 2003. Influence of the Arctic oscillation and El Niño-Southern oscillation (ENSO) on ice conditions in the Baltic Sea: the wavelet approach. J Geophys Res Atmos. 108 (D21).

Kisi, O., 2015. An innovative method for trend analysis of monthly pan evaporations. J Hydrol. 527, 1123-1129.

Li, B., Chen, Y., Shi, X., Chen, Z., Li, W., 2013. Temperature and precipitation changes in different environments in the arid region of northwest China. Theor Appl Climatol. 112(3-4), 589-596.

Li, B.F, Chen Y.N., Chen, Z.S., Xiong, H., & Lian, L., 2016. Why does precipitation in northwest China show a significant increasing trend from 1960 to 2010. Atmos Res 167: 275-284.

Li, C.H., 2003. Summary of Studies on Drought and Rainstorm in Northwest China. J Arid Meteorol. (01):1-7. (in Chinese)

Li, Z., He, Y., Theakstone, W.H., Wang, X., Zhang, W., Cao, W., ... & Chang, L., 2012. Altitude dependency of trends of daily climate extremes in southwestern China, 1961–2008. J Geograph Sci. 22(3), 416-430. (in Chinese)

Li, Z., He, Y., Wang, C., Wang, X., Xin, H., Zhang, W., Cao, W., 2011. Spatial and temporal trends of temperature and precipitation during 1960–2008 at the Hengduan Mountains, China. Quat Int. 236(1-2), 127-142.

Liu, Q., Yang, Z., Cui, B., 2008. Spatial and temporal variability of annual precipitation during 1961–2006 in Yellow River Basin, China. J Hydrol. 361(3-4), 330-338.

Meng, Q., Bai, H.Y., Guo, S.Z., 2020. Based on the spatio-temporal changes of precipitation in the Qinling region of Anusplin over the past 50 years. J Soil water Conserv, 1-7 [2020-01-10] (in Chinese)

Mohan, P., Srinivas, C., Yesubabu, V., Baskaran, R., Venkatraman, B., 2018. Simulation of a heavy rainfall event over Chennai in Southeast India using WRF: Sensitivity to microphysics parameterization. Atmos Res. 210, 83–99.

Mohorji, A.M., Şen, Z., Almazroui, M., 2017. Trend analyses revision and global monthly temperature innovative multi-duration analysis. Earth Syst Environ. 1(1), 9.

Öztopal, A., Şen, Z., 2017. Innovative trend methodology applications to precipitation records in Turkey. Water Resour manag. 31(3), 727-737.

Özger, M., MiṠ, hraand A.K., Singh, V.P., 2010. Scaling characteristics of precipitation data in conjunction with wavelet analysis. J Hydrol. 395 (3), 279–288.

Proud, S.R., Rasmussen, L.V., 2011. The influence of seasonal rainfall upon Sahel vegetation. Remote Sens Lett. 2 (3), 241–249.

Qin, J., Bai, H.Y., Zhai, D.P., Wang, J., Li, S.H., Li, B., 2017. Relationship between Tree Ring Width of Abies fargesii and Climate Factors in Niubeiliang Nature Reserve in Eastern Qinling Mountains. J Glaciol Geocryl. 39(03), 540-548. (in Chinese)

Şen, Z., 2012. Innovative trend analysis methodology. J Hydrol Eng. 17 (9), 1042–1046.

Şen, Z., 2017. Innovative trend significance test and applications. Theor Appl Climatol. 127 (3–4), 1–9.

Torrence, C., Compo, G.P., 1998. A practical guide to wavelet analysis. Bull. Am. Meteorol. Soc. 79 (1), 61–78.

Torrence, C., Webster, P.J., 1999. A comparison of satellite and in situ-based sea surface temperature climatologies. J. Clim. 12 (12), 1848–1863.

Von, S.H., 1995. Misuses of statistical analysis in climate research//Analysis of climate variability. Springer, Berlin, Heidelberg, 1999, 11-26.

Wang, X., Wang, B., Xu, X., 2019. Effects of large-scale climate anomalies on trends in seasonal precipitation over the Loess Plateau of China from 1961 to 2016. Ecol Indic. 107, 105643.

Wang, R., Ren, H., Ouyang, Z., 2000. China Water Vision (Beijing: China Meteorological Press).

Wang, Y., Xu, Y., Tabari, H., Wang, J., Wang, Q., Song, S., & Hu, Z., 2020. Innovative trend analysis of annual and seasonal rainfall in the Yangtze River Delta, eastern China. Atmos Res. 231, 104673.

Wu, H., Qian, H., 2017. Innovative trend analysis of annual and seasonal rainfall and extreme values in Shaanxi, China, since the 1950s. Int J Climatol. 37(5), 2582-2592.

Wu, Y., Wu, S.Y., Wen, J., Xu, M., & Tan, J., 2016. Changing characteristics of precipitation in China during 1960–2012. Int J Climatol. 36(3), 1387-1402.

Xiao, M., Zhang, Q., Singh, VP., 2015. Influences of ENSO, NAO, IOD and PDO on seasonal precipitation regimes in the Yangtze River basin, China. Int J Climatol. 35(12), 3556–3567.

Xu, Z.X., Li, J.Y., Liu, C.M., 2007. Long - term trend analysis for major climate variables in the Yellow River basin. Hydrol Process. 21(14), 1935-1948.

Yang, Y., Guan. H., Batelaan, O., Mcvicar, T.R., Long, D., Piao, S., Liang, W., Liu, B., Jin, Z., Simmons, C., 2016. Contrasting responses of water use efficiency to drought across global terrestrial ecosystems. Sci Rep. 6, 1–8.

Yang, Q., Ma, Z., Xu, B., 2017. Modulation of monthly precipitation patterns over East China by the Pacific Decadal Oscillation. Clim Change. 144, 1–13.

Yu, H., Wang, L., Yang, R., Yang, M., & Gao, R., 2018. Temporal and spatial variation of precipitation in the Hengduan Mountains region in China and its relationship with elevation and latitude. Atmos Res. 213, 1-16.

Zhang, Y., Tian, Q., Guillet, S., Stoffel, M., 2017. 500-yr. precipitation variability in Southern Taihang Mountains, China, and its linkages to ENSO and PDO. Climatic Change. 144(3), 419-432.

Zhang, Q., Peng, J., Singh, V.P., Li, J., & Chen, Y. D., 2014. Spatio-temporal variations of precipitation in arid and semiarid regions of China: the Yellow River basin as a case study. Global and Planetary Change. 114, 38-49.

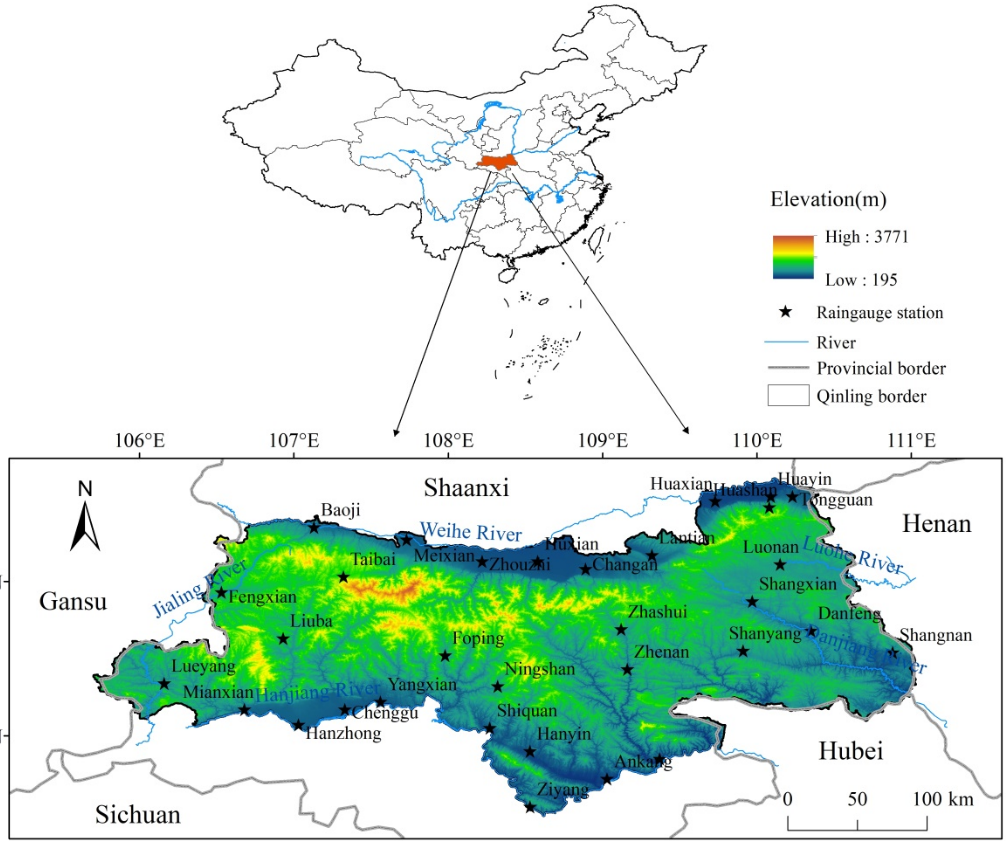

Fig. 1 The location of the Qinling Mountains.

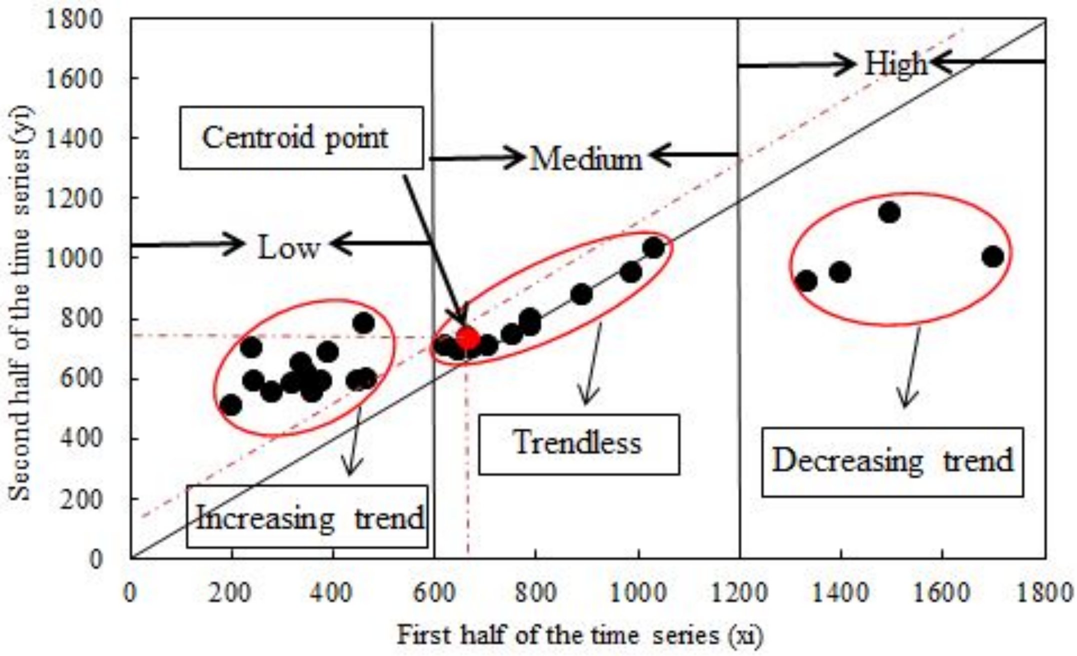

Fig. 2 Illustration of the Innovative Trend Analysis (ITA) method.

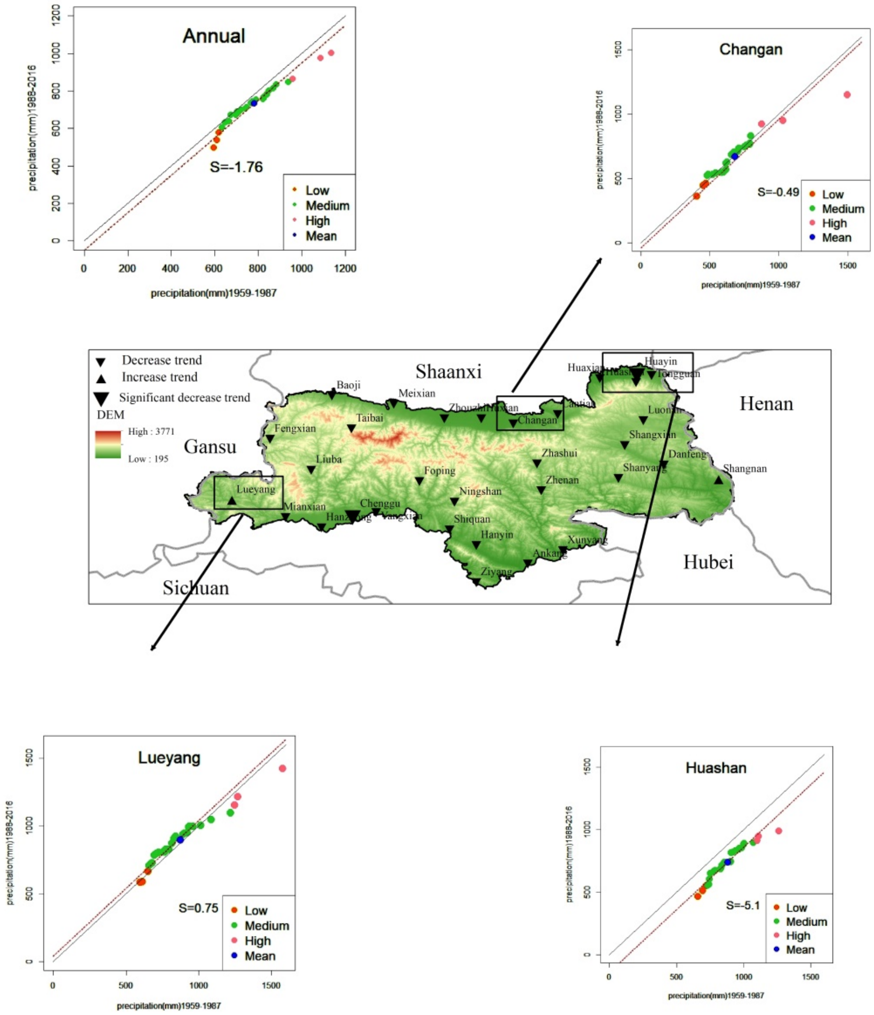

Fig. 3 Results of the trend for annual precipitation by ITA method.

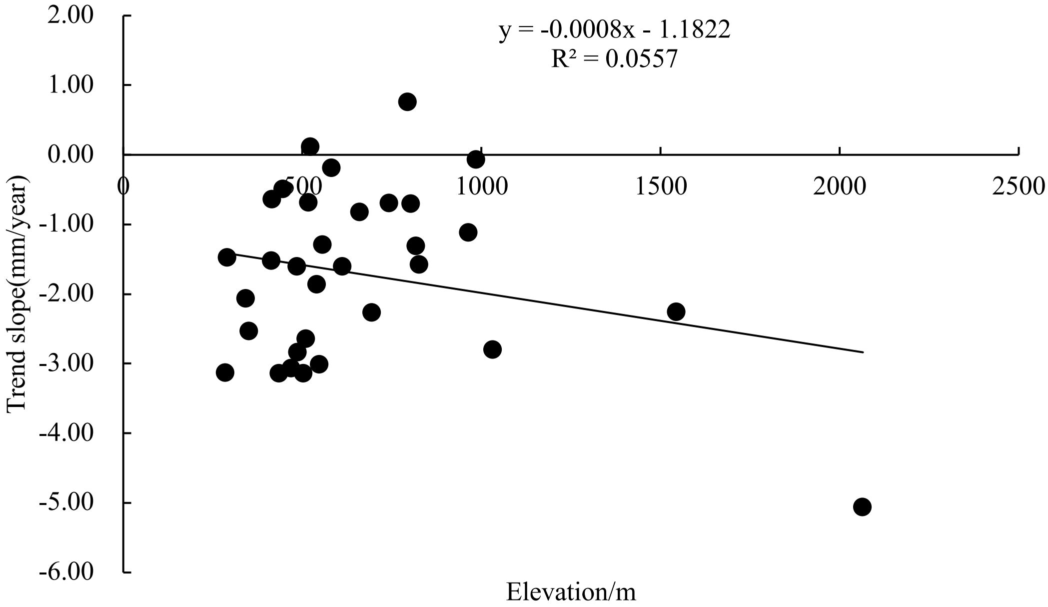

Fig. 4 Annual precipitation trend slope changes with altitude

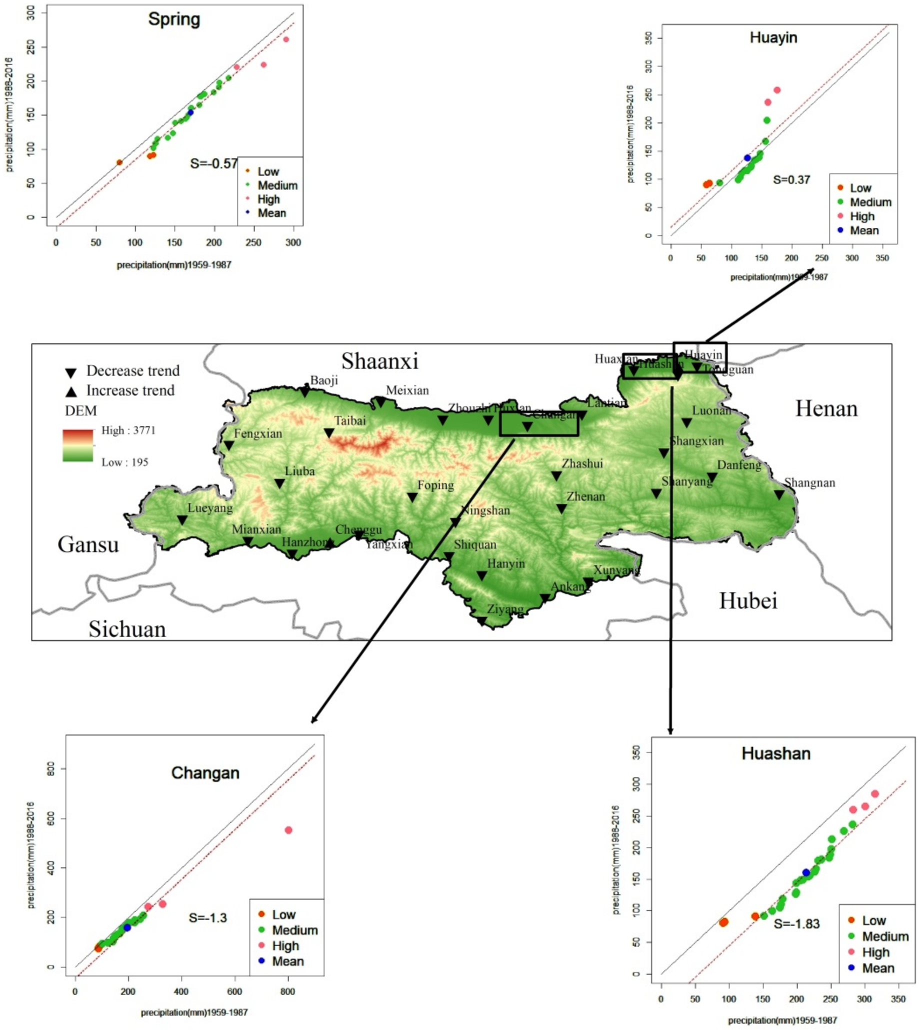

Fig. 5 Results of the trend for spring precipitation by ITA method.

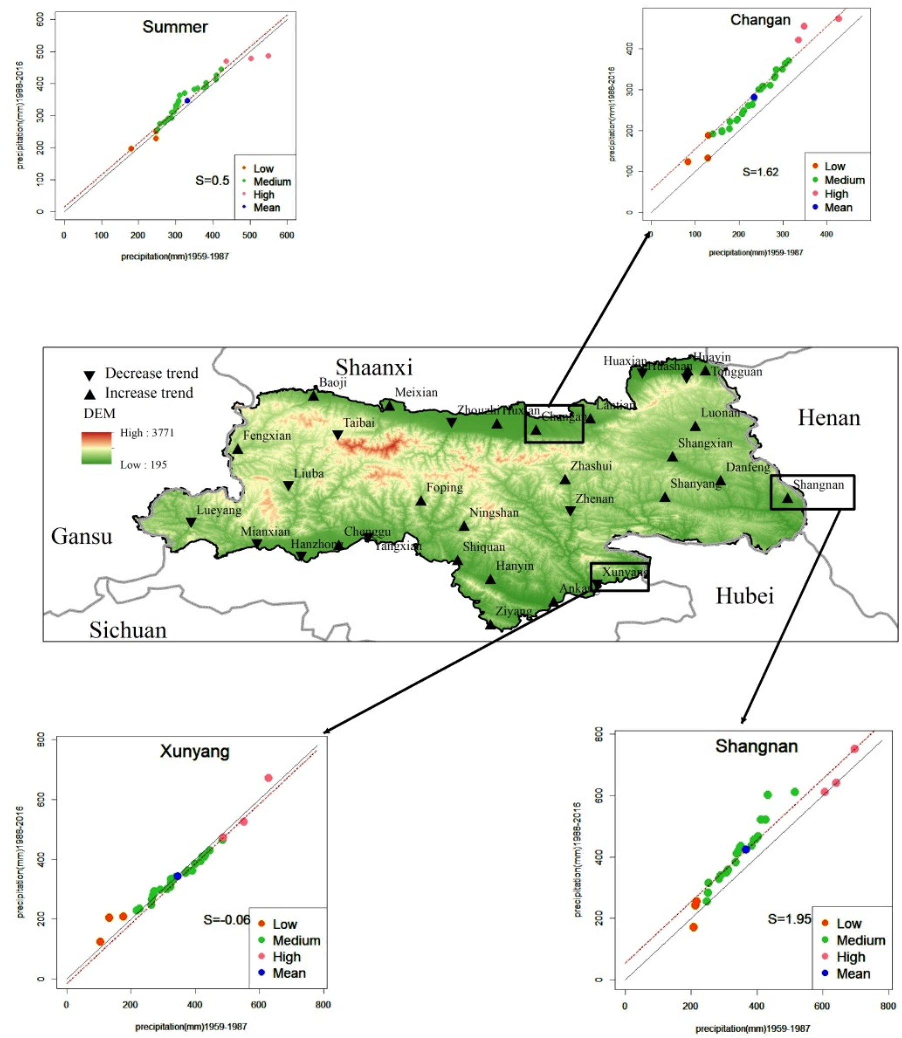

Fig. 6 Results of the trend for summer precipitation by ITA method.

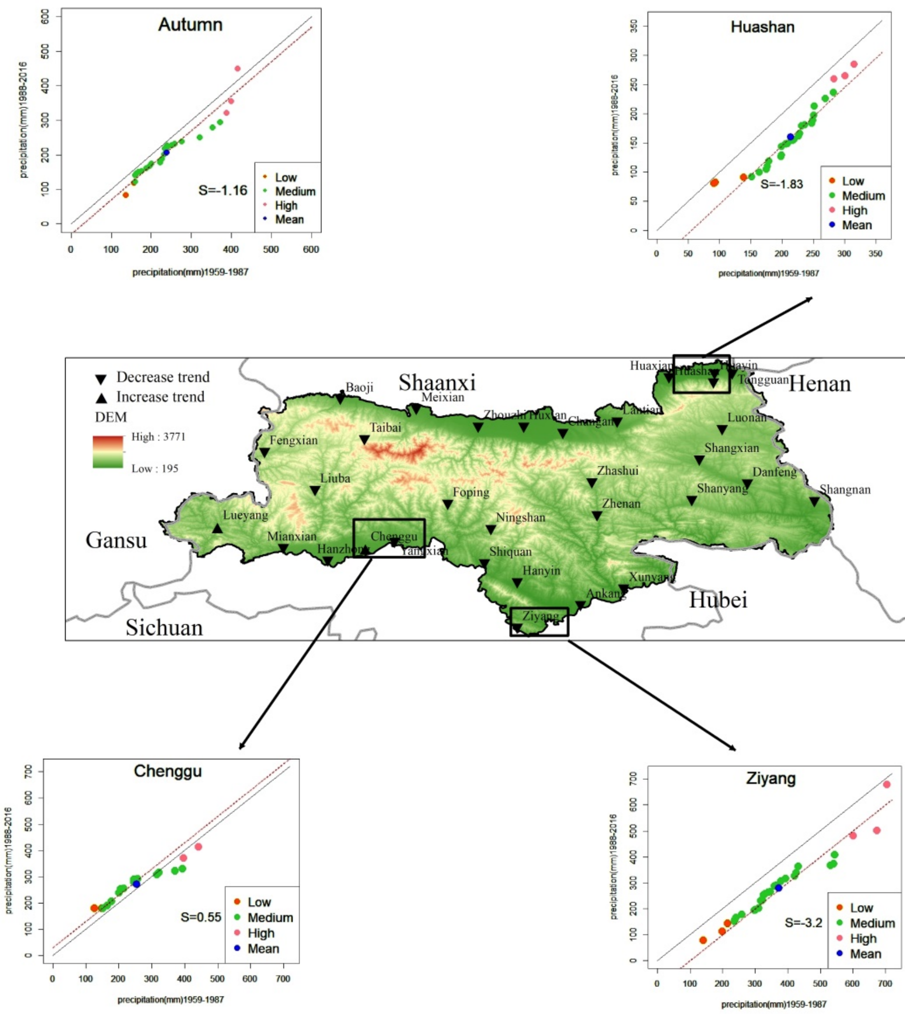

Fig. 7 Results of the trend for autumn precipitation by ITA method.

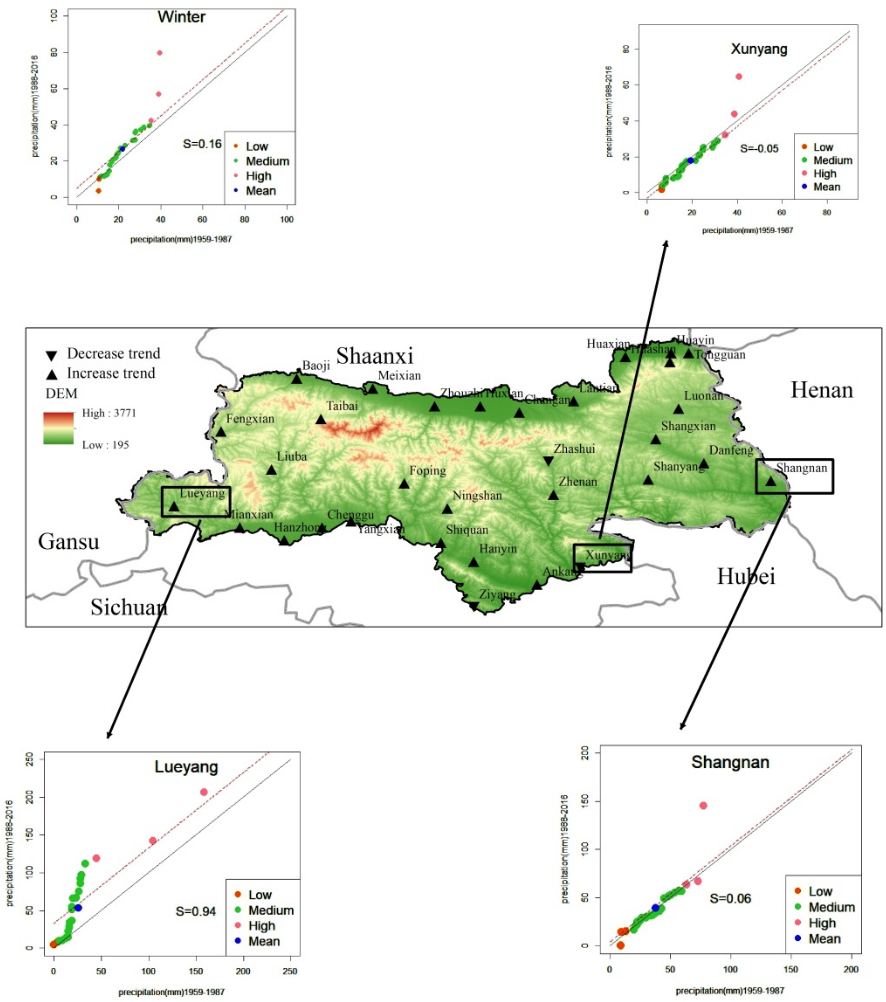

429

430 Fig. 8 Results of the trend for winter precipitation by ITA method.

431

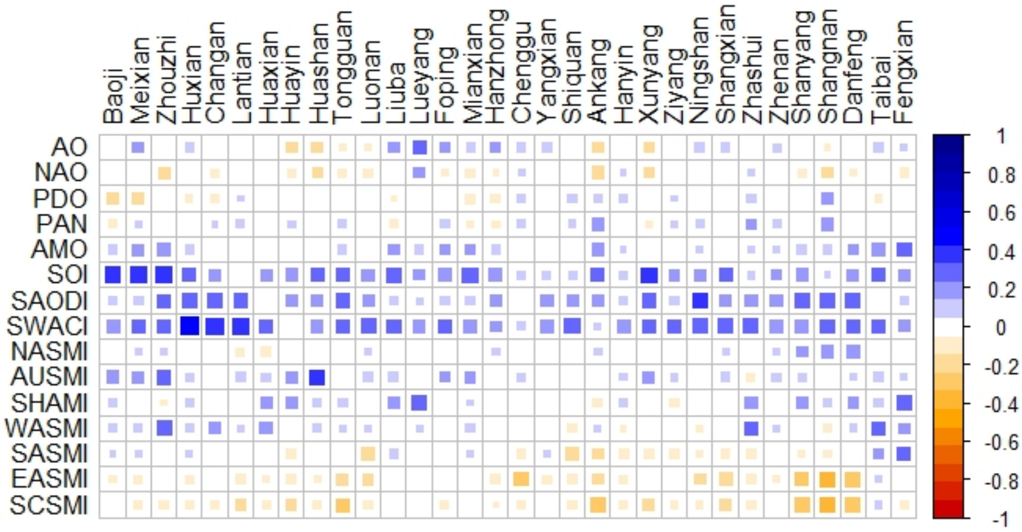

Fig. 9 Result of correlation coefficients between annual precipitation of 32 stations and climate indices on annual precipitation

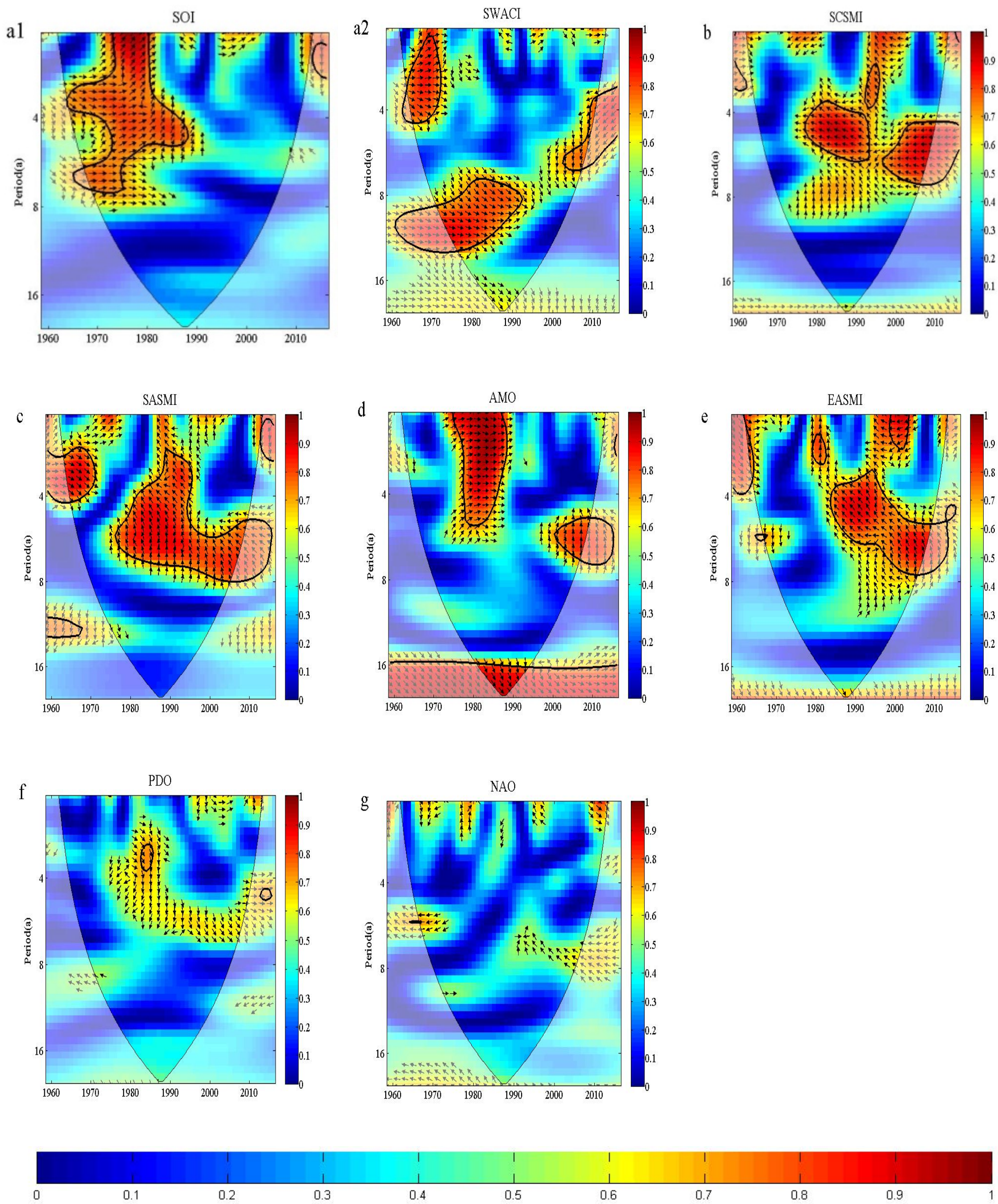

Fig. 10 Result of WTC between annual precipitation and different climate anomalies indices. (The thick black contours depict the 5% significant level, and the black line is the cone of influence. Right-pointing arrows indicate that the two signals are in phase while left-pointing arrows are for anti-phase signals. Down-pointing arrows denote that the PRE are ahead of the climate index, whereas up-pointing arrows mean that the PRE lag behind the climate index.)

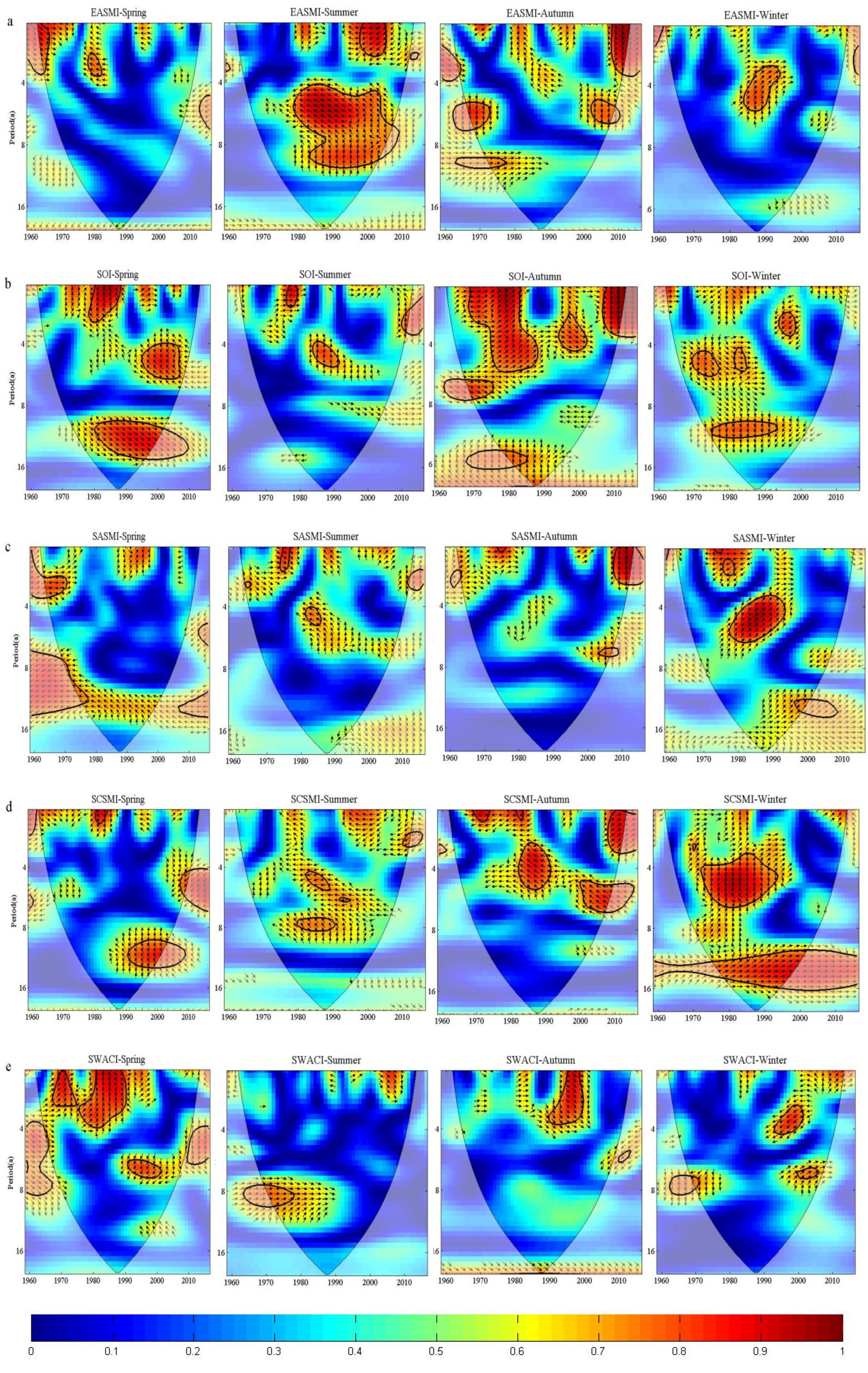

Fig. 11 Result of WTC between seasonal precipitation and 5 climate indices.